Radiocarbon, Vol 64, Nr 5, 2022, p 1139–1158 DOI:10.1017/RDC.2022.55


# IMPLICATIONS OF SINGLE-STEP GRAPHITIZATION FOR RECONSTRUCTING LATE HOLOCENE RELATIVE SEA-LEVEL USING RADIOCARBON-DATED ORGANIC COASTAL SEDIMENT

Juliet P Sefton[1]* • Andrew C Kemp[1] • Kathryn L Elder[2] • Roberta L Hansman[2] • Mark L Roberts[2]

[1]Department of Earth and Ocean Sciences, Tufts University, Medford, MA 02155, USA
[2]National Ocean Sciences Accelerator Mass Spectrometry Facility, Woods Hole Oceanographic Institution, Woods Hole, MA 02543, USA

**ABSTRACT.** Late Holocene relative sea-level reconstructions are commonly generated using proxies preserved in salt-marsh and mangrove sediment. These depositional environments provide abundant material for radiocarbon dating in the form of identifiable macrofossils (salt marshes) and bulk organic sediment (mangroves). We explore if single-step graphitization of these samples in preparation for radiocarbon dating can increase the number and temporal resolution of relative sea-level reconstructions without a corresponding increase in cost. Dating of salt-marsh macrofossils from the northeastern United States and bulk mangrove sediment from the Federated States of Micronesia indicates that single-step graphitization generates radiocarbon ages that are indistinguishable from replicates prepared using traditional graphitization, but with a modest increase in error (mean/maximum of 6.25/15 additional $^{14}$C yr for salt-marsh macrofossils). Low $^{12}$C currents measured on bulk mangrove sediment following single-step graphitization likely render them unreliable despite their apparent accuracy. Simulated chronologies for six salt-marsh cores indicate that having twice as many radiocarbon dates (since single-step graphitization costs ~50% of traditional graphitization) results in narrower confidence intervals for sample age estimated by age-depth models when the additional error from the single-step method is less than ~50 $^{14}$C yr (~30 $^{14}$C yr if the chronology also utilizes historical age markers). Since these thresholds are greater than our empirical estimates of the additional error, we conclude that adopting single-step graphitization for radiocarbon measurements on plant macrofossils is likely to increase precision of age-depth models by more than 20/10% (without/with historical age markers). This improvement can be implemented without additional cost.

**KEYWORDS:** age-depth model, mangrove, Massachusetts, Micronesia, salt marsh.

## INTRODUCTION

Detailed and near-continuous reconstructions of relative sea level (RSL) change during the late Holocene (past ~3000 years) offer insight into the response of sea level to climate variability (e.g., Kopp et al. 2016; Kemp et al. 2018; Gehrels et al. 2020). These proxy records demonstrated that the centennial-scale rate of regional and global sea-level rise since the late 19th century is consistent with climate trends and without precedent in at least 3000 years (Kopp et al. 2016; Walker et al. 2021). At mid- to high latitudes, salt marshes are the primary sedimentary archive used to reconstruct late Holocene RSL (e.g., Gerlach et al. 2017; Gehrels et al. 2020) and there are increasing efforts to utilize mangrove sediments at low latitudes in this capacity (e.g., Woodroffe et al. 2015a). The history of sediment accumulation is established by an age-depth model that leverages the stratigraphic relationship between dated depths in a single core (Blaauw and Christen 2011; Parnell and Gehrels 2015; Wright et al. 2017). The organic nature of salt-marsh and mangrove sediment provides ample material for radiocarbon dating of identifiable macrofossils (such as *in-situ* stems and rhizomes of salt-marsh plants) or bulk sediment (common for mangroves; e.g., Woodroffe et al. 2015b). Radiocarbon dating is often supplemented by historical markers, which are pollution and land-use trends of known age and provenance recognized in downcore profiles of elemental abundance, isotopic activity, and pollen (Marshall 2015). Efforts to increase the temporal resolution of late Holocene RSL reconstructions, coupled with growing recognition that replication within and among sites

*Corresponding author. Email: juliet.sefton@monash.edu

is a pre-requisite for distinguishing local- and regional-scale RSL trends will require an increased number of radiocarbon dates (and therefore cost).

The National Ocean Sciences Accelerator Mass Spectrometry (NOSAMS) facility recently developed a new "single-step" method (Elder et al. 2019) to convert samples of organic carbon into graphite for subsequent measurement of radiocarbon by accelerator mass spectrometry (AMS). Briefly (see Elder et al. 2019 for a complete description), a sample and catalysts are placed in a tube that is evacuated, sealed, and baked in a furnace (with a capacity of ~80 tubes). In contrast, the traditional (hydrogen reduction) method of graphitization employed at NOSAMS requires sample combustion and collection of $CO_2$ in a tube on one line followed by manual transfer of each tube to a second line (the graphite reactor; Gagnon et al. 2000), resulting in a daily capacity of up to 20 samples per operator. The single-step method requires significantly less handling and fewer materials than the traditional method, resulting in a ~50% cost reduction to end users and up to a four-fold increase in daily throughput of samples per operator. Previous comparisons of radiocarbon measurements on standard samples such as oxalic acid, historic tree rings of known age, and swipe samples processed using both single-step and traditional graphitization indicated comparable accuracy, but with a modest increase in measurement error for the single-step method (Elder et al. 2019).

We investigate the potential for single-step graphitization to increase the number and resolution of late Holocene RSL reconstructions developed from salt-marsh and mangrove sediment without a corresponding increase in cost. First, we compare radiocarbon measurements from replicate samples processed at NOSAMS using the single-step and traditional graphite reduction methods. The samples analyzed are plant macrofossils from a core of salt-marsh sediment collected in Massachusetts, USA and bulk mangrove sediment from cores collected on two islands in the Federated States of Micronesia with contrasting geomorphologies. Comparison of results for each core quantifies the relative accuracy, precision, and reliability of the single-step method. Second, we simulate chronologies developed with single-step graphitization by building cost-neutral age-depth models from subsets of published dates in six salt-marsh cores with varied accumulation histories. These simulations assume that the ~50% reduction in cost for each radiocarbon date is reinvested by dating twice as many samples with increased error in radiocarbon measurements. Uncertainties in the simulated age-depth models are compared to threshold values established in our empirical evaluation of radiocarbon ages from samples that underwent single-step and traditional graphitization.

## STUDY SITES

The Short Beach salt marsh is located in Winthrop, Massachusetts (at 42°23'24"N, 70°53'24"W) and displays a pattern of vegetation that is characteristic of salt marshes in the northeastern United States (Bertness 1991; Redfield 1972). Tidal flats are unvegetated and the low salt-marsh floral zone is narrow and vegetated by *Spartina alterniflora*. The expansive high salt-marsh platform is occupied by a peat-forming community of *Spartina patens* and *Distichlis spicata*. Great diurnal tidal range (mean lower low water to mean higher high water) is 3.13 m. The core selected for analysis is comprised ~4 m of high salt-marsh sediment that accumulated under sustained RSL rise driven by ongoing glacio-isostatic adjustment over the late Holocene at a rate of ~0.9 mm/yr (Peltier 1996; Engelhart and Horton 2012; Piecuch et al. 2018). These continuous sequences of high salt-marsh peat

https://doi.org/10.1017/RDC.2022.55 Published online by Cambridge University Press

are ideal for reconstructing RSL because they accumulated in a narrow elevational range and indicate that the salt-marsh surface tracked RSL rise through time. Furthermore, they usually contain abundant and identifiable plant macrofossils for radiocarbon dating (Niering et al. 1977).

Mangrove forests are the dominant ecosystem on low-energy coasts in the Federated States of Micronesia. On the steep-sided, volcanic island of Pohnpei, the estuarine mangrove forest at Nanitipw (at 6°57'00"N, 158°13'48"E) is vegetated by *Rhizophora apiculata, Bruguiera gymnorrhiza*, *Sonneratia alba*, and *Xylocarpus granatum,* with most coastal fringes occupied by *Rhizophora stylosa*. Great diurnal tidal range is 0.88 m. The stratigraphy beneath the site is estuarine silt overlain by ~4 m of organic-rich silt (carbonate is rare in this unit) that accumulated in a mangrove forest during the past ~5000 years (Fujimoto et al. 1995; Athens and Stevenson 2012) in response to sustained RSL rise. Kosrae is also a volcanic island and the study site at Pukusruk (at 5°21'00"N, 163°1'12"E) is a mangrove forest on the open coast vegetated by *Rhizophora apiculata*, *Bruguiera gymnorrhiza*, and *Sonneratia alba*. Great diurnal tidal range is 1.17 m. The stratigraphy underlying the site is coral substrate overlain by ~2 m of organic silt (carbonate is rare in this unit) that accumulated in a mangrove environment during the past ~2000 years (Kanawa et al. 1995; Fujimoto et al. 1996). In both cores, macrofossils are rarely preserved and are usually roots rather than material that could be reliably interpreted as having formed, or been deposited on, a paleo-mangrove surface (e.g., leaves). Published radiocarbon ages from the two study sites are from bulk mangrove sediment. A scarcity or absence of macrofossils with reliable relationships to paleo surfaces is a common characteristic of late Holocene mangrove sediment in many regions (e.g., Ellison 1993; Sefton et al. 2021; Woodroffe et al. 2015b).

## METHODS

### Sample Selection

The cores of salt-marsh peat and mangrove sediment were recovered in overlapping, 50-cm long sections using a Russian corer to prevent compaction and contamination during collection. They were stored in rigid plastic sleeves and refrigerated until analysis. The Short Beach core was dissected to isolate *in-situ* and identifiable plant macrofossils (stems and rhizomes of the common high salt-marsh grasses *Distichlis spicata* and *Spartina patens*), with known relationships to paleo salt-marsh surfaces (Niering et al. 1977; van de Plassche et al. 1998; Donnelly 2006). From this suite of material, we selected depths with large enough samples to generate replicate radiocarbon dates and to provide approximately even coverage of the core from 0.5 m to 4.0 m. After examining cores from Nanitipw and Pukusruk at the time of collection and finding very few macrofossils, we sliced the collected cores into 1-cm thick increments to provide a suite of bulk-sediment samples for radiocarbon dating from which depths were selected to provide an approximately even down-core distribution.

### Sample Preparation and Treatment

Identifiable plant macrofossils found in growth position in the Short Beach core were isolated from the sediment matrix and soaked in deionized and organic-free (MilliQ) water to loosen adhered sediment. Under a binocular microscope any remaining sediment was removed along with plant material that was not part of the target macrofossil (e.g., younger ingrowing rootlets; Kemp et al. 2013b). Samples underwent acid-base-acid pretreatment by adding 10–15 mL of

10% HCl. They were left to digest for three hours before being washed to neutral pH with MilliQ water. Approximately 20 mL of 2% NaOH solution was added to each sample and heated in a water bath at 70°C for 30 minutes. This step was repeated until the supernatant remained clear upon addition of more NaOH solution, after which the sample was washed to neutral pH with MilliQ water. Approximately 10–15 mL of 10% HCl was added to the samples and left for one hour before washing to neutral pH with MilliQ water. Samples were then oven dried at 40°C.

Bulk mangrove sediment from Nanitipw and Pukusruk was sieved with MilliQ water to retain the fraction <500 μm and remove large root fragments that are likely to be anomalously young (Kemp et al. 2019; Woodroffe et al. 2015b). This step ensured that the retained sediment was well mixed (homogenized). Water added to the sample during sieving was removed under vacuum to concentrate the sediment onto a glass fiber filter. The sediment was oven dried at 40°C and then transferred into a test tube for acid-only pretreatment. Approximately 10–15 mL of 10%, HCl was added to each sample and they were left to digest for three hours. An acidity of <4 pH was typically achieved by the first acid wash, which indicated a complete reaction (and removal of any carbonates). Samples were washed to neutral pH with MilliQ water and then oven dried at 40°C.

After pretreatment, each sample was divided into two subsamples of approximately equal mass. Each subsample was weighed into a pre-ashed silver capsule and submitted to NOSAMS, where one replicate was converted to graphite using the single-step method and one replicate followed the traditional method.

### Conversion to Graphite and Radiocarbon Measurement

The pretreated replicate samples for traditional graphitization were combusted at high temperature and the resulting gas was captured and sealed in a quartz tube (Gagnon et al. 2000). Each tube was then manually transferred and cracked to release the gas into a vacuum system where $CO_2$ was purified and quantified before being introduced to a reactor for reduction to graphite using Fe catalyst in the presence of excess hydrogen (Vogel et al. 1987). The pretreated, replicate samples for single-step graphitization were loaded into assembled, prebaked Pyrex tubes with reagents (Elder et al. 2019). The assembled tubes were placed in a muffle furnace for three hours at 500°C and a further four hours at 550°C, during this step graphite formed in the tubes. All graphite was pressed into aluminum cathodes and analyzed on the Continuous Flow AMS system (CFAMS; Roberts et al. 2010). Blank corrections were applied following a formula that fits the observed mass dependency in measured fraction modern carbon of quality control samples (Roberts et al. 2019).

### Simulated Age-Depth Models

We explore the effect of adopting single-step graphitization by generating age-depth models using published chronological data from six salt marshes in eastern North America that represent a spectrum of late Holocene accumulation histories (Table 1). Each site has downcore chronological data from a relatively high concentration of uncalibrated radiocarbon dates (all generated by converting macrofossils of common salt-marsh plants to graphite using the traditional method at NOSAMS) and recognition of historical trends and events in pollution and land-use. The number and nature of these markers varies among the six sites. We use reported radiocarbon ages and their uncertainties (i.e., $^{14}C$ yr

Table 1 Cores of salt-marsh sediment used to simulate chronologies. The mean uncertainty for sample age is the 95% credible interval for the control chronologies that included radiocarbon dates and historical age markers.

| Site | Reference | Depth (m) | Max $^{14}C$ age | Number of radiocarbon dates/marker horizons | Mean uncertainty for sample-age (years) |
|---|---|---|---|---|---|
| Big River, Newfoundland | Kemp et al. (2018) | 2.91 | 2705 ± 41 | 42/7 | 133 |
| East River, CT | Kemp et al. (2015) | 2.31 | 2080 ± 40 | 15/14 | 136 |
| Cape May Courthouse, NJ | Kemp et al. (2013a) | 2.08 | 1350 ± 30 | 13/17 | 98 |
| Sand Point, NC | Kemp et al. (2011, 2017) | 2.99 | 2420 ± 35 | 19/10 | 128 |
| Nassau Landing, FL | Kemp et al. (2014) | 1.25 | 2420 ± 25 | 10/14 | 177 |
| Little Manatee, FL | Gerlach et al. (2017) | 1.20 | 2180 ± 15 | 16/6 | 186 |

BP and ± $^{14}C$ yr rather than fraction modern) because this is the result that end users typically evaluate and employ in age-depth models. Since ages are rounded following the conventions of Stuiver and Polach (1977) before being reported by NOSAMS they are inherently less precise than the underlying radiocarbon measurements. For each core we divided the available radiocarbon dates into two populations (from even and odd numbered depths) under the premise that a radiocarbon determination made following single-step graphitization (currently) costs ~50% of the traditional method at NOSAMS. For the odd/even populations an age-depth history was generated using Bchron (Haslett and Parnell 2008; Parnell et al. 2008). In generating a history of sediment accumulation, Bchron calibrates reported radiocarbon dates; we use the IntCal20 calibration (Reimer et al. 2020) in all analyses. The predicted ages and uncertainties (95% credible interval) for each 1-cm thick interval of the core were then averaged across the two (odd/even depths) age-depth models. This step was first performed using only radiocarbon ages as input for the age-depth models and was then repeated with inclusion of all available historical chronological markers. We refer to these results as *control chronologies* because they represent accumulation histories developed using existing protocols (traditional graphitization).

We next simulated chronologies generated using the single-step method by using all available radiocarbon ages as input for the age-depth models, but we added extra error to each reported radiocarbon age in increments of 5 $^{14}C$ yr from 0 to 75. For every 1-cm thick increment of the core, we calculated the difference in predicted age and age error (number of years spanned by the 95% credible interval for sample age) between each simulation and the corresponding control chronology. These differences measure the effect of adopting a cost-neutral approach to building core chronologies because there are twice as many samples processed using the single-step method, which has greater error than the traditional method (but at approximately half the cost).

https://doi.org/10.1017/RDC.2022.55 Published online by Cambridge University Press

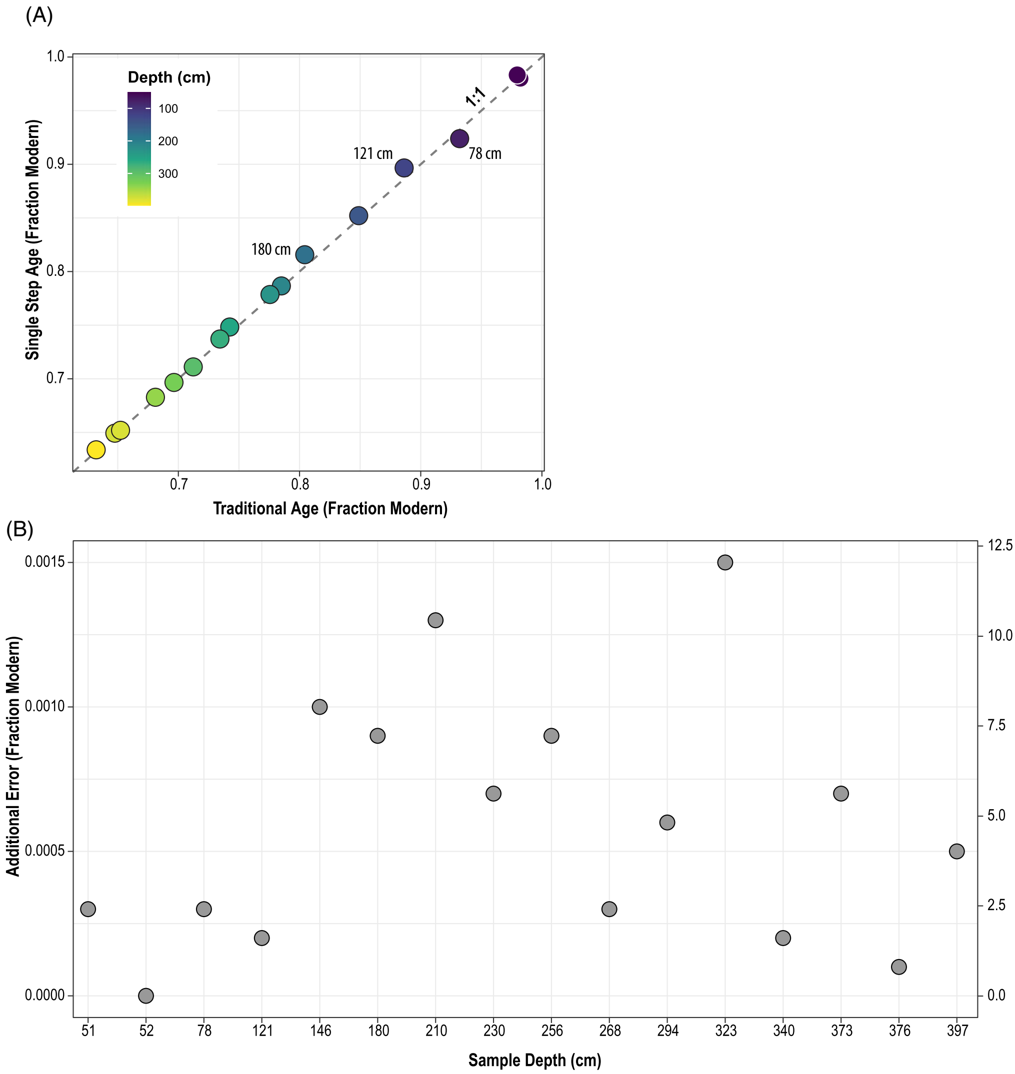


Figure 1 Replicate radiocarbon ages from a core of salt-marsh peat collected at Short Beach. (A) Correlation of radiocarbon ages from replicate samples processed using the single-step and traditional methods for converting organic samples to graphite. Bi-directional (1σ) uncertainties are smaller than symbols. Symbol color denotes depth in core and demonstrates the stratigraphic ordering of samples. (B) Difference in reported radiocarbon error for samples processed using the single-step and traditional methods for graphitization. Positive values indicate a larger error for the single-step method. The difference expressed in radiocarbon years is a direct conversion of the fraction modern values. (See online version for color figures.)

## RESULTS

### Salt-Marsh Macrofossils

Rhizomes and stems of *Distichlis spicata* or *Spartina patens* from 16 depths in the core of salt-marsh sediment from Short Beach were prepared for radiocarbon analysis. Following pretreatment, each sample was divided into two replicates for single-step and traditional graphitization (Figure 1; Supporting Table 1 in Supplementary Material). Radiocarbon

https://doi.org/10.1017/RDC.2022.55 Published online by Cambridge University Press

ages are stratigraphically ordered and range from 0.632 fraction modern (FM) to 0.982 FM for traditional graphitization (equivalent to 3680–145 $^{14}C$ yr BP) and 0.634–0.983 FM for single-step graphitization (equivalent to 3660–135 $^{14}C$ yr BP). There is an excellent agreement between radiocarbon measurements from single-step and traditional graphitization of replicate samples (Figure 1A). For 13 out of 16 depths, replicate radiocarbon measurements are indistinguishable from one another within their 1σ reported errors. Of the three remaining depths, single-step graphitization resulted in two instances of younger ages (at 121 cm and 180 cm) and one older age (at 78 cm) compared to the traditional method. Radiocarbon measurements on samples converted to graphite using the single-step method have systematically larger uncertainties than those from the traditional method. The additional error ranges from 0 to 0.0015 FM (equivalent to 0–12 $^{14}C$ yr) with a mean of 0.0006 FM (~5 $^{14}C$ yr; Figure 1B).

### Bulk Mangrove Sediment

Replicate radiocarbon measurements from four depths in the Nanitipw core follow stratigraphic ordering and the ages ranged from 0.707 to 0.979 FM when processed using the traditional methods (equivalent to 2785–170 $^{14}C$ yr BP) and 0.716 to 0.979 FM under the single-step method (equivalent to 2684–170 $^{14}C$ yr BP; Figure 2A; Supporting Table 1 in Supplementary Material). At two depths (40 cm and 165 cm), replicate measurements were indistinguishable from one another within 1σ errors, but at the two other depths (240 cm and 365 cm) samples that underwent single-step graphitization yielded younger ages. Radiocarbon uncertainties were larger for the single step method by 0.0018–0.0039 FM (equivalent to ~15–35 $^{14}C$ yr; Figure 2B).

A further four bulk sediment samples from the mangrove core at Pukusruk were analyzed in the same way (Supporting Table 1 in Supplementary Material). This sequence of sediment is relatively young with ages ranging from 0.955 to 0.984 FM for traditional graphitization (equivalent to 369–132 $^{14}C$ yr BP) and 0.957 to 0.985 for the single-step method (equivalent to 351–121 $^{14}C$ yr BP; Figure 2A). The radiocarbon measurements do not adhere to stratigraphic ordering. At three depths (35 cm, 91 cm, and 119 cm) ages following traditional and single-step graphitization overlap within their 1σ uncertainties, while the remaining sample (at 63 cm) yielded an age that was 0.0062 FM younger for the single-step method (equivalent to ~50 $^{14}C$ yr). Radiocarbon measurements were more uncertain following single step preparation by 0.0014–0.0018 FM (equivalent to ~12 $^{14}C$ yr; Figure 2B). Among all samples of bulk mangrove sediment, the mean increase in error during radiocarbon measurement was 0.0023 FM (equivalent to ~18 $^{14}C$ yr).

## DISCUSSION

### Reliability and Precision

Single-step graphitization results in radiocarbon measurements that have systematically larger uncertainties than those made on replicate samples prepared using the traditional method. For salt-marsh macrofossils the difference is modest, with a mean of 0.0006 FM and maximum of 0.0015 FM (Figure 2D). The mean/maximum additional error in reported radiocarbon ages for the same samples is 6.25 and 15 $^{14}C$ yr, respectively. In contrast, the additional error for bulk mangrove sediment was greater (mean of 0.0023 FM; maximum of 0.0039 FM), with mean reported errors being 21.25 $^{14}C$ yr greater (range of 15–40 $^{14}C$ yr). For replicate samples of standards and historic wood, Elder et al. (2019) attributed the larger error to less efficient

https://doi.org/10.1017/RDC.2022.55 Published online by Cambridge University Press

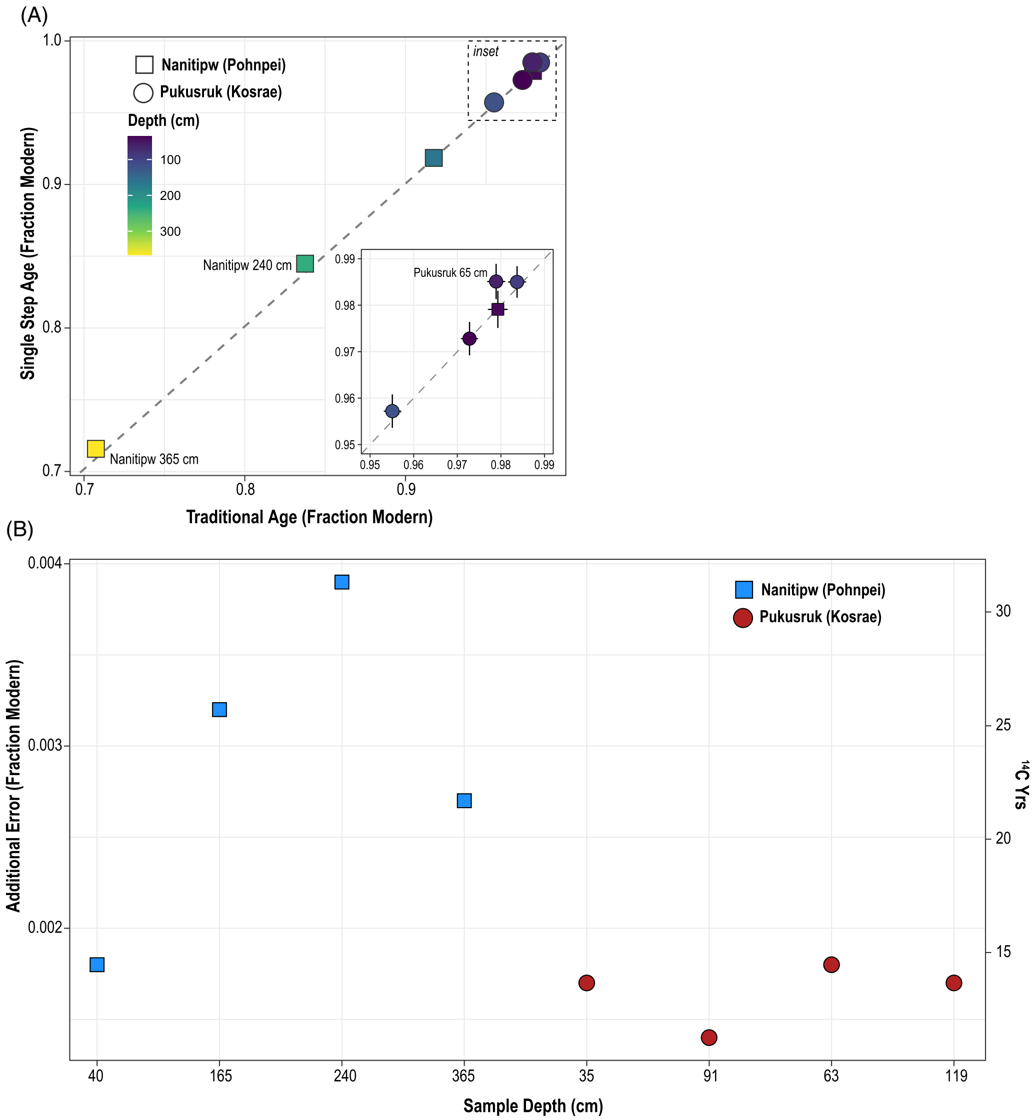


Figure 2 Replicate radiocarbon ages from cores of mangrove sediment in the Federated States of Micronesia collected from Nanitipw on Pohnpei and Pukusruk on Kosrae. (A) Correlation of radiocarbon ages from replicate samples processed using the single-step and traditional methods for converting organic samples to graphite. Bi-directional (1σ) uncertainties are smaller than symbols. Symbol color denotes depth in core and demonstrates the stratigraphic ordering of samples. Symbol shape differentiates results from Nanitipw and Pukusruk. (B) Difference in reported radiocarbon error for samples processed using the single-step and traditional methods for graphitization. Positive values indicate a larger error for the single-step method. The difference expressed in radiocarbon years is a direct conversion of the fraction modern values. (See online version for color figures.)

conversion of organic carbon to graphite by the single-step method, as evidenced by an average 42% reduction in $^{12}C$ current measured by the AMS. Reduced $^{12}C$ current causes larger scatter and reduced counting statistics, resulting in larger error. We evaluate measured $^{12}C$ currents to

https://doi.org/10.1017/RDC.2022.55 Published online by Cambridge University Press

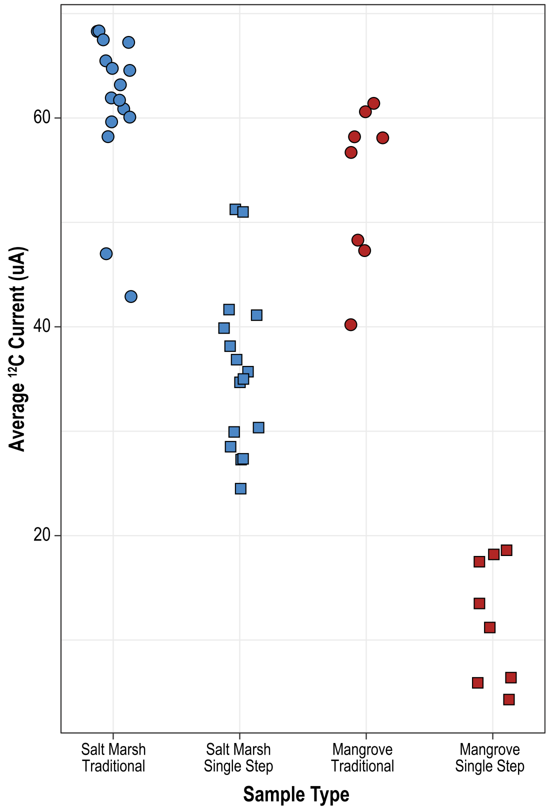


Figure 3 $^{12}C$ current measured by the accelerator mass spectrometer. Data are grouped by sample type (salt-marsh macrofossils from Short Beach and mangrove sediment from Nanitipw and Pukusruk) and the method used for conversion to graphite (single step or traditional). For clarity of presentation, individual data points are horizontally jittered to reduce overlap. (See online version for color figures.)

investigate if and how reduced yields during single-step graphitization influence radiocarbon error and age.

The $^{12}C$ current measured in the ion source on salt-marsh macrofossil and bulk mangrove sediment samples is systematically reduced for samples that underwent single-step graphitization (Figure 3). For salt-marsh macrofossils, mean measured $^{12}C$ current was 61.4 μA (range of 42.9–68.3 μA) for the traditional method compared to 35.8 μA (range of 24.5–51.2 μA) for the single-step method. For individual depths, the mean reduction in $^{12}C$ current was 40.4% (ranging from –8.5% to 58.3%), which is consistent with results reported by Elder et al. (2019). Among all samples of bulk mangrove sediment, mean $^{12}C$ current fell from 53.9 μA (range 40.2–61.4 μA) using the traditional method to 12.0 μA (range of 4.3–18.6 μA) for the single-step method. For individual samples, the mean reduction in $^{12}C$ current was 78.7% (range 67.2–89.3%), which is considerably larger than the change we observed for salt-marsh macrofossils and the materials studied by Elder et al. (2019).

https://doi.org/10.1017/RDC.2022.55 Published online by Cambridge University Press

The very low $^{12}C$ current measured on bulk mangrove sediment that underwent single-step graphitization may occur for two reasons. Firstly, the relatively complex and heterogenous composition of bulk sediment compared to macrofossils likely decreases the efficiency and predictability of reactions during graphitization resulting in reduced yields (Elder et al. 2019). Secondly, regardless of the method used to convert organic carbon to graphite, bulk mangrove sediment generates lower $^{12}C$ current than salt-marsh macrofossils (Figure 3), possibly due to its lower concentration of organic carbon (mean of ~13%, compared to ~47% for the salt-marsh macrofossils) (Elder et al. 2019). Given the very low $^{12}C$ currents, we consider the radiocarbon measurements from bulk mangrove sediment that underwent single-step graphitization to be unreliable. Although these results appear accurate when compared to those from traditional graphitization (Figure 2), such corroborating evidence is unavailable in most circumstances. Further experimentation (e.g., changing the type and amount of catalysts and reagents) is underway at NOSAMS to refine the single-step method to improve yields from graphitization of bulk organic sediment samples (Elder et al. 2019). However, such changes may need to be made on a case-by-case basis given the likely variability in the composition of bulk organic sediment across space and through time.

The error of radiocarbon measurements increases in a non-linear fashion as $^{12}C$ current decreases (Figure 4A). Across salt-marsh macrofossils and bulk mangrove sediment, current reductions less than ~40% resulted in uncertainties that were ~5 $^{14}C$ yr greater, but current reductions greater than ~75% caused radiocarbon uncertainties to more than double in some instances and to exceed an additional 20 $^{14}C$ yr in three instances. Differences in sample age under single-step and traditional graphitization hint that greater fractionation of carbon isotopes may occur during single-step graphitization if yields are particularly reduced/low (Figure 4B). Of the five samples with current reductions less than 40%, only one generated a mean radiocarbon age that was older using the single-step method than the traditional method. In contrast, single-step graphitization resulted in an older mean radiocarbon age for 18 of the 19 samples with current reductions greater than 40%. However, the magnitude of this effect appears modest even at extremely low yields and in all but two cases is less than the uncertainty in age difference for individual samples. Similarly, Elder et al. (2019) showed that single-step graphitization of oxalic acid resulted in $^{13}C/^{12}C$ values 10% more depleted than those from traditional graphitization of replicate samples. Although those measurements agreed within their 2σ uncertainties, samples that underwent single-step graphitization remained ~0.5 ‰ more enriched in radiocarbon (or younger) than consensus values.

We conclude that single-step graphitization of salt-marsh macrofossils results in radiocarbon measurements that are accurate (or at least as accurate as those from the traditional method) and reliable (reduced, but acceptable yields during graphitization), but slightly more uncertain (additional <15 $^{14}C$ yr). For bulk mangrove sediment, very low yield arising from low organic content and complex composition results in large inflation of uncertainties and renders the dates unreliable despite apparent accuracy (in the absence of the replicate results from the traditional method). We did not prepare any bulk salt-marsh peat (or mangrove macrofossils) for radiocarbon dating and therefore cannot evaluate definitively if the unreliable results arose from the environment of deposition (mangrove vs salt marsh) or sample type (bulk sediment vs macrofossil). However, the likely explanations of relatively low organic content coupled with complex and heterogenous composition suggest that sample type is the cause and that bulk organic sediment from other

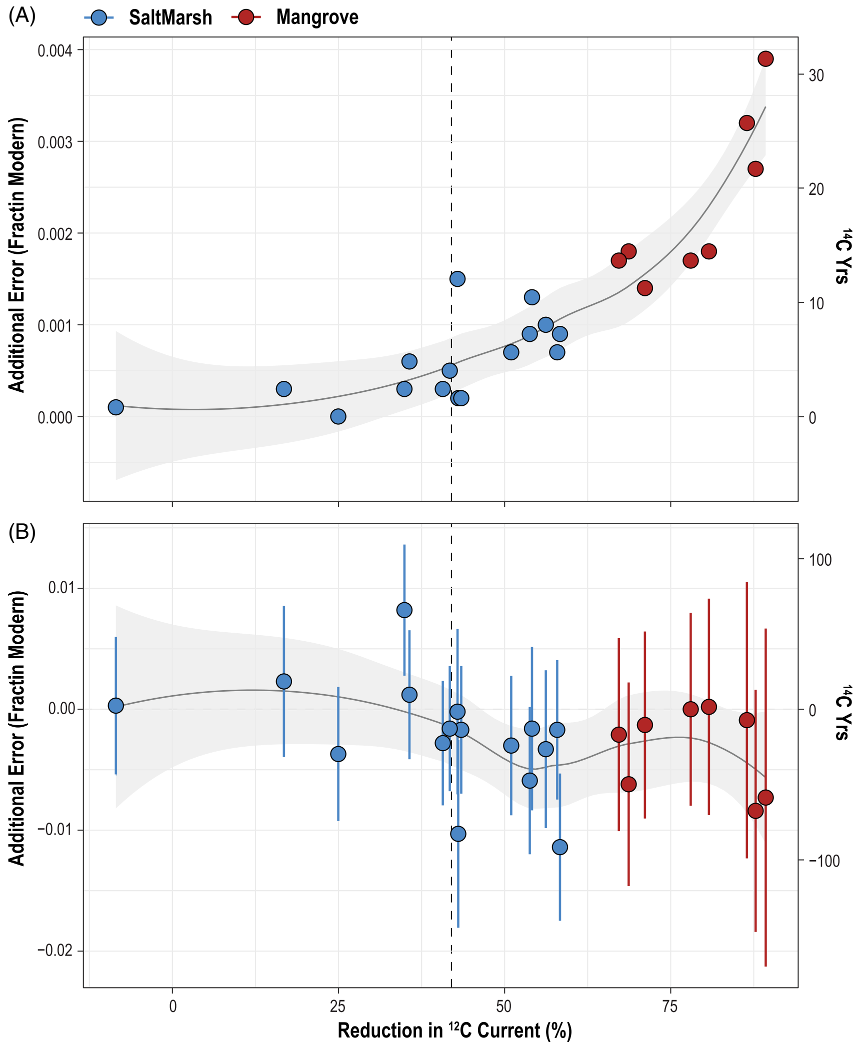


Figure 4 Correlation between $^{12}C$ current measured by the accelerator mass spectrometer and (A) the additional error of radiocarbon measurements (FM = fraction modern) associated with single-step graphitization in comparison to the traditional method; and (B) difference in age arising from the two different methods. Negative values indicate that the single-step method resulted in an older age than the traditional method. Solid line and shaded envelope are a LOESS best fit. The dashed line represents the 42% average reduction reported by Elder et al. (2019) because of less efficient conversion of organic carbon to graphite. (See online version for color figures.)

depositional environments (including salt marshes) may also return unreliable radiocarbon ages when prepared using single-step graphitization. Further optimization of the single-step method is required for future use with bulk sediment from mangroves and other settings.

## Building Sediment Chronologies for Near-Continuous Relative Sea-Level Reconstructions

Efforts to produce near-continuous reconstructions of late Holocene RSL change using organic coastal sediment rely on constraining sedimentation histories using age-depth models

https://doi.org/10.1017/RDC.2022.55 Published online by Cambridge University Press

(e.g., Wright et al. 2017; Kemp et al. 2018; Gehrels et al. 2020). From an input dataset of uncalibrated radiocarbon ages and marker horizons at discrete depths, the model estimates the age of each depth in the core (usually 1-cm thick intervals) with uncertainty. We investigated if single-step graphitization could decrease uncertainties in age-depth models in a cost-neutral fashion to facilitate more reliable detection of RSL changes on sub-centennial timescales by comparing the control and simulated chronologies from six sites along the North American Atlantic coast (Table 1). Our analysis was restricted to salt-marsh sites where the radiocarbon-dated material was macrofossils since single-step graphitization of bulk sediment may not result in high enough yields for the measurements to be considered independently reliable (Figures 3 and 4). We adopt two thresholds from the empirical comparison of radiocarbon measurements on salt-marsh macrofossils for evaluating the likely effect of adopting single-step graphitization (Figure 1B). These thresholds are the mean (6.25 $^{14}$C yr) and maximum (15 $^{14}$C yr) increase in reported error. Output from the age-depth models are sample age and uncertainty in calendar year.

For chronologies developed only from radiocarbon dates on plant macrofossils, there is little difference in the estimated age of 1-cm thick samples between the control and simulated chronologies at all six sites (Figure 5, left column). When the reported radiocarbon error is inflated by 15 $^{14}$C yr (the maximum difference observed in the empirical data from Short Beach; Figure 1B), the mean difference in sample age between the control and simulated chronologies varies from –2 years (at Big River) to 7 years (at Nassau Landing). One standard deviation of the age difference ranges from 4 years East River to 11 years at Little Manatee. Similarly, for chronologies that also utilize historical age markers, the mean age difference between control and simulated chronologies is small and not systematic (Figure 6, left column). With reported radiocarbon errors inflated by 15 $^{14}$C yr, the mean difference in sample age ranged from –3 years at East River to 4 years at Sand Point. One standard deviation of the age difference ranged from 4 years at Cape May Courthouse to 11 years at Little Manatee. Across all sites and samples, there is no indication that the mean age of a sample is biased by single-step graphitization when estimated using age-depth models, unless the radiocarbon certainty is inflated by at least 50–60 $^{14}$C yr (Figure 7A), which our empirical comparison indicates is highly unlikely for salt-marsh macrofossils of late Holocene age (Figure 4A). This result arises because only the error of the radiocarbon age was changed. This presumption is supported by results from Short Beach, which indicate that single-step graphitization does not bias radiocarbon ages on salt-marsh plant macrofossils (Figure 4B).

There is a systematic decrease in the uncertainty of sample ages estimated by age-depth models where twice as many radiocarbon ages are used as input. When only radiocarbon ages (i.e., no historical age markers) constitute the input (Figure 5, right column) and reported radiocarbon error is inflated by 5 $^{14}$C yr (similar to the mean difference between single-step and traditional ages of 6.25 $^{14}$C yr observed in the empirical data from Short Beach; Figure 1B), the mean (across all depths in a core) width (number of years) of the 95% credible interval for estimated sample age is reduced by 15.5% (at Little Manatee) to 38.5% (at Nassau Landing). Across all sites and samples, the reduction is 25% (Figure 7B). Inflating the radiocarbon error by 15 $^{14}$C yr (the maximum difference between single-step and traditional graphitization observed at Short Beach; Figure 1B), results in age-depths models that are 15–34% more precise for single sites (at Big River and Nassau respectively) and 21% across all sites.

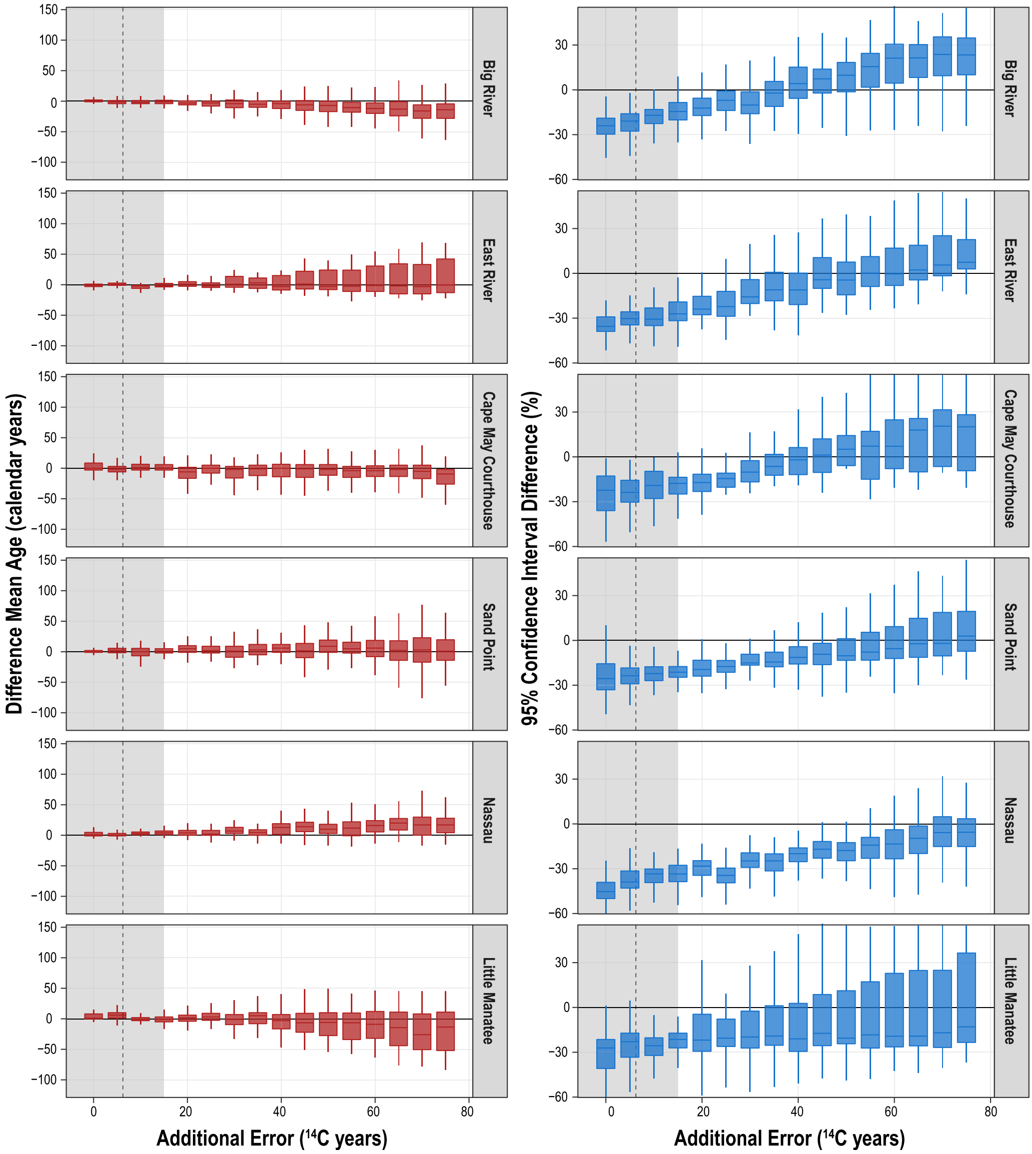


Figure 5 Difference between control and simulated chronologies at six salt marshes in eastern North America (organized geographically from north to south). The control chronologies included approximately half of the published radiocarbon measurements with their reported uncertainties. The simulated chronologies utilized all radiocarbon measurements, but added additional error at five-year increments. Historical age markers were not used. Left column is the difference in mean sample age, where positive/negative values indicate that age in a simulated chronology is older/younger than age in the corresponding control chronology. Right column is the difference in width of the 95% credible interval expressed as a percentage difference compared to the control chronologies. Negative values indicate that the error is reduced in the simulated chronologies. Dashed vertical line and shaded envelope represent, respectively, the mean (6.25 $^{14}$C yr) and range (≤15 $^{14}$C yr) of observed differences in radiocarbon error between single-step and traditional graphitization of salt-marsh plant macrofossils. Box plots represent the median (solid horizontal line), 25th and 75th percentiles (hinges), and the largest value no further than 1.5 times the interquartile range from the hinge (approximately a 95% confidence interval for comparing medians; whiskers). Some 95% confidence intervals extend beyond plot limits for clarity of presentation. (See online version for color figures.)

https://doi.org/10.1017/RDC.2022.55 Published online by Cambridge University Press

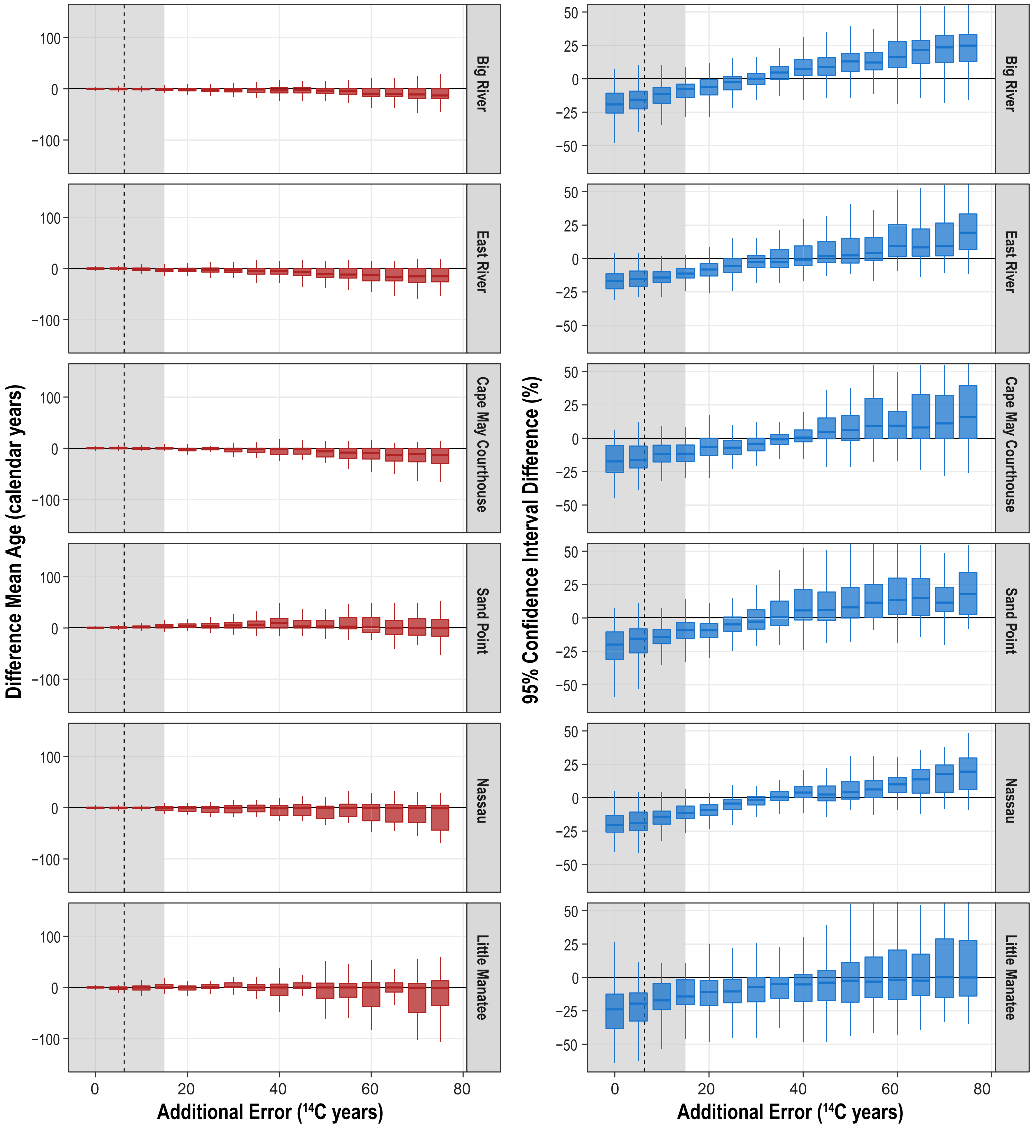


Figure 6 Difference between control and simulated chronologies at six salt marshes in eastern North America (organized geographically from north to south). The control chronologies included approximately half of the published radiocarbon measurements with their reported uncertainties and all available historical age markers. The simulated chronologies utilized all radiocarbon measurements, but added additional error at five-year increments. All historical age markers were retained and used in the simulated chronologies with their original uncertainties. Left column is the difference in mean sample age, where positive/negative values indicate that age in a simulated chronology is older/younger than age in the corresponding control chronology. Right column is the difference in width of the 95% credible interval expressed as a percentage difference compared to the control chronologies. Negative values indicate that the error is reduced in the simulated chronologies. Dashed vertical line and shaded envelope represent, respectively, the mean (6.25 $^{14}$C yr) and range (≤15 $^{14}$C yr) of observed differences in radiocarbon error between single-step and traditional graphitization of salt-marsh plant macrofossils. Box plots represent the median (solid horizontal line), 25th and 75th percentiles (hinges), and the largest value no further than 1.5 times the interquartile range from the hinge (approximately a 95% confidence interval for comparing medians; whiskers). Some 95% confidence intervals extend beyond plot limits for clarity of presentation. (See online version for color figures.)

https://doi.org/10.1017/RDC.2022.55 Published online by Cambridge University Press

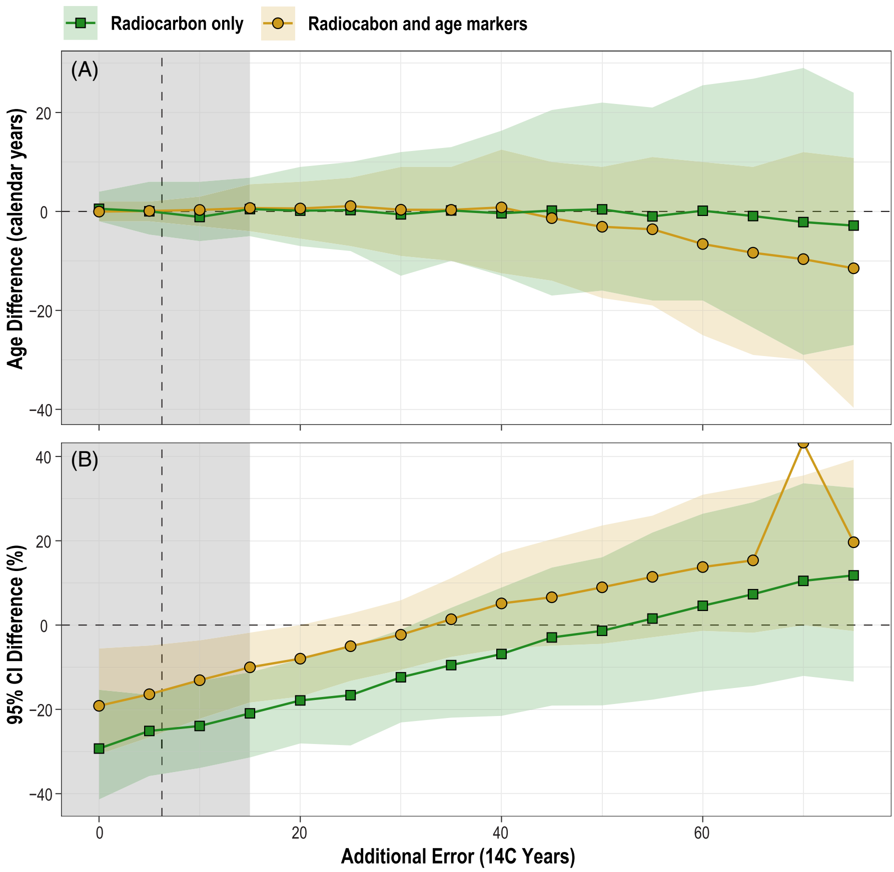


Figure 7 Comparison of control and simulated chronologies averaged across all sample depths in the six cores of salt-marsh sediment from eastern North America. (A) Difference in age where positive/negative values indicate that age in a simulated chronology is older/younger than age in the corresponding control chronology. (B) Difference in width of the 95% credible interval expressed as a percentage difference compared to the control chronologies. Negative values indicate that the uncertainty is reduced in the simulated chronologies. Series color distinguishes chronologies that did and did not include historical age markers, shaded regions represent the 68% credible interval. Dashed vertical line and shaded envelope represent, respectively, the mean (6.25 $^{14}$C yr) and range (≤15 $^{14}$C yr) of observed differences in radiocarbon error between single-step and traditional graphitization of salt-marsh plant macrofossils. (See online version for color figures.)

A similar pattern occurs in chronologies that include historical markers as input to the age-depth model, but the reduction in the width of the 95% credible interval for sample age is less pronounced. With radiocarbon error increased by 5 $^{14}$C yr, the improvement in precision was 15–22% for single sites (at East River and Little Manatee respectively; Figure 6, right column) and 16% across all sites and samples (Figure 7B). With radiocarbon error inflated by 15 $^{14}$C yr, the average improvement in precision was 8–12% for single sites (at Little Manatee and Cape May Courthouse respectively) and 10% across all sites. The smaller improvement for age-models that incorporate historical markers arises because these input ages are usually very precise (a specific calendar year in the case of peak $^{137}$Cs activity for example; Corbett and Walsh 2015). Despite being restricted to the upper

https://doi.org/10.1017/RDC.2022.55 Published online by Cambridge University Press

(shallow) section of sediment cores that represent the historical period (Marshall 2015), marker horizons influence age estimates and their uncertainties at lower depths when chronologies (such as those from Bchron) are developed using repeated, equiprobable sampling of stratigraphically ordered samples (Parnell and Gehrels 2015; Wright et al. 2017). In effect, the presence of historical markers narrows the pool of plausible age-depth relationships and diminishes the sensitivity of age-depth models to the size of radiocarbon uncertainties at depth.

A convenient measure of when single-step graphitization is likely to cease generating age-depth models with narrower 95% credible intervals for sample age is to identify when the mean change in precision becomes positive. For chronologies developed using only radiocarbon, this occurs when reported radiocarbon errors are inflated by at least 40 $^{14}$C yr (at Big River) and in the case of Little Manatee and Nassau Landing is at more than 75 $^{14}$C yr (Figure 5, right column). For chronologies that also include historical markers, this threshold is reached with a smaller increase in radiocarbon error (but at least 30 $^{14}$C yr; Figure 6, right column). Given that the maximum observed increase in reported radiocarbon error is just 15 $^{14}$C yr, we conclude that radiocarbon dating twice as many salt-marsh plant macrofossils is likely to result in a more precise age-depth model when compared to chronologies using fewer, more precise radiocarbon ages. Therefore, adopting single-step graphitization for building chronologies of salt-marsh peat accumulation is advantageous over continuing to use the traditional method. This advantage can be delivered at no additional cost to the end user (although additional sample submissions could potentially increase turnaround times at some radiocarbon laboratories).

A caveat to our conclusion is that that the empirical thresholds we established through comparison of radiocarbon ages on replicate samples were derived from macrofossils of *Spartina patens* and *Distichlis spicata*. These are the dominant salt-marsh grasses between approximately Delaware and Massachusetts on the Atlantic coast of North America. From Virginia southward, the dominant salt-marsh grass is *Juncus roemerianus* (Eleuterius 1976), although even here *Distichlis spicata* is often disproportionately radiocarbon dated because of its robust preservation (Kemp et al. 2017). Salt marshes in Maine and the Canadian Maritimes are often characterized by a more diverse flora that includes *Juncus gerardii* and *Triglochin* sp. (Scott et al. 1981; Daly et al. 2007; Johnson et al. 2007). Although it is possible that the increase in radiocarbon error from single-step graphitization is species (and therefore location) dependent, we contend that the relatively high organic content and homogeneity of salt-marsh plant macrofossils regardless of species (Gabriel and de la Cruz 1974; Wang et al. 2003; Kemp et al. 2010) is likely to ensure that the yield from single-step graphitization is sufficiently high to cause only a modest increase in error. Therefore, our results from Short Beach are probably applicable to efforts to establish salt-marsh accumulation histories by radiocarbon dating plant macrofossils across a wide range of salt-marshes in eastern North America (such as those used for simulating chronologies; Table 1, Figures 5 and 6) and other regions (e.g., Gehrels et al. 2006; Long et al. 2012) despite their floral diversity. Likewise, paleoenvironment reconstructions from other sedimentary environments (e.g., peatlands) that utilize radiocarbon dating of plant macrofossils to build age-depth models for cores (e.g., Swindles et al. 2010; Kołaczek et al. 2019) may achieve improved chronological precision by adopting single-step graphitization.

## CONCLUSIONS

A fundamental step in producing near-continuous, late Holocene RSL reconstructions from salt-marsh and mangrove sediment is constraining the history of sedimentation for a core. This task is usually performed by applying an age-depth model to radiocarbon-dated plant macrofossils or bulk sediment and historical age markers from discrete depths with known stratigraphic relationships to one another. Increasing the number and resolution of detailed RSL reconstructions therefore requires more radiocarbon dates. However, adopting single-step graphitization presents an opportunity to increase the precision of age-depth models without a corresponding increase in cost. We compared replicate radiocarbon measurements following single-step and traditional graphitization of salt-marsh macrofossils from a core collected in Massachusetts and bulk mangrove sediment from cores collected on Pohnpei and Kosrae (Federated States of Micronesia). Replicate radiocarbon ages were largely indistinguishable from one another, but single-step graphitization results in larger radiocarbon error (mean increase of 6.25 $^{14}$C yr for salt-marsh macrofossils) because of reduced yield. For mangrove sediment the yield following single-step graphitization was too low (as evidenced by $^{12}$C currents on the ion source) to produce radiocarbon measurements that can be considered independently reliable. This problem is likely to arise in bulk sediment with relatively low organic content and heterogenous composition from other depositional environments (including salt marshes).

We simulated chronologies for six cores of salt-marsh peat at sites in eastern North America (Newfoundland to Florida) to investigate the likely impact of adopting single-step graphitization, which enables researchers to have approximately twice as many radiocarbon-dated depths in a core at no extra cost, but with larger error for each date. This analysis suggests that if the additional error from single-step graphitization of macrofossils does not exceed ~30 $^{14}$C yr (for cores with historical age markers), then the resulting age-depth model can be made more precise with no increase in cost over continuing to use traditional graphitization of about half as many samples. Despite regional differences in taxa, the increased radiocarbon error for plant macrofossil samples prepared by single-step graphitization (≤15 $^{14}$C yr) observed in Massachusetts is likely representative of late Holocene macrofossils from salt marshes in other regions and in other depositional environments (e.g., peatlands and mangroves). We therefore anticipate that age-depth models are likely to be >20% more precise for chronologies constrained only by radiocarbon ages and >10% more precise for chronologies that also include historical age markers. The more modest improvement identified in chronologies that include historical age markers arises from the tight limitations they place on the age of shallow sediment, which subsequently influences sedimentation histories in older, deeper parts of the core.

## SUPPLEMENTARY MATERIAL

To view supplementary material for this article, please visit https://doi.org/10.1017/RDC.2022.55.

## ACKNOWLEDGMENTS

This work was supported by National Science Foundation (NSF) awards OCE-1831382, OCE-2002431, and OCE-1942563, as well as by NSF NOSAMS cooperative agreement OCE-1755125. Jack Ridge participated in fieldwork at Short Beach and we thank Simon Engelhart (supported by NSF award OCE-1831405), Byron Halavik, Madeline Varney, Maxim, and Yosta for their assistance in collecting the mangrove cores from Pohnpei and Kosrae. Access to Nanitipw was made possible by Saimon Lihpai (Pohnpei Forestry Service). We are grateful to Blair Charley (Kosrae Island Resource Management Authority) for facilitating access to field sites on Kosrae. We thank Robin Edwards and an anonymous reviewer for providing thoughtful comments that helped to improve this manuscript.

## REFERENCES

Athens JS, Stevenson J. 2012. Pohnpei coring records: the natural distribution of *cyrtosperma chamissonis*. Journal of Pacific Archaeology 3(1):14.

Bertness MD. 1991. Zonation of *spartina patens* and *spartina alterniflora* in New England salt marsh. Ecology 72(1):138–148.

Blaauw M, Christen JA. 2011. Flexible paleoclimate age-depth models using an autoregressive gamma process. Bayesian Analysis 6(3):457–474, 418.

Corbett DR, Walsh JP. 2015. $^{210}$lead and $^{137}$cesium: establishing a chronology for the last century. In: Shennan I, Long AJ, Horton BP, editors. Handbook of sea level research. Chichester: John Wiley & Sons. p. 361–372.

Daly JF, Belknap DF, Kelley JT, Bell T. 2007. Late holocene sea-level change around newfoundland. Canadian Journal of Earth Sciences 44(10): 1453–1465.

Donnelly JP. 2006. A revised late holocene sea-level record for northern Massachusetts, USA. Journal of Coastal Research. 22(5):1051–1061.

Elder KL, Roberts ML, Walther T, Xu L. 2019. Single step production of graphite from organic samples for radiocarbon measurements. Radiocarbon 61(6):1843–1854.

Eleuterius L. 1976. The distribution of *juncus roemerianus* in the salt marshes of North America. Chesapeake Science 17(4):289–292.

Ellison JC. 1993. Mangrove retreat with rising sea-level, Bermuda. Estuarine, Coastal and Shelf Science 37(1):75–87.

Engelhart SE, Horton BP. 2012. Holocene sea level database for the atlantic coast of the united states. Quaternary Science Reviews 54:12–25.

Fujimoto K, Miyagi T, Kikuchi T. 1995. Formative and maintainable mechanisms of mangrove habitats in micronesia and the phillipines. In: Miyagi T, editor. Rapid sea level rise and mangrove habitat. Gifu University. p. 91–98.

Fujimoto K, Miyagi T, Kikuchi T, Kawana T. 1996. Mangrove habitat formation and response to holocene sea-level changes on kosrae island, micronesia. Mangroves and Salt Marshes 1(1):47–57.

Gabriel BC, de la Cruz AA. 1974. Species composition, standing stock, and net primary production of a salt marsh community in mississippi. Chesapeake Science 15(2):72–77.

Gagnon AR, McNichol AP, Donoghue JC, Stuart DR, von Reden K, Hayes NJM, Schneider R, Elder K, Bellino M, Long P. 2000. The nosams sample preparation laboratory in the next millenium: Progress after the woce program. Nuclear Instruments and Methods in Physics Research Section B: Beam Interactions with Materials and Atoms 172(1–4):409–415.

Gehrels WR, Dangendorf S, Barlow N, Saher M, Long A, Woodworth P, Piecuch C, Berk K. 2020. A preindustrial sea-level rise hotspot along the Atlantic coast of North America. Geophysical Research Letters 47(4):e2019GL085814.

Gehrels WR, Szkornik K, Bartholdy J, Kirby JR, Bradley SL, Marshall WA, Heinemeier J, Pedersen JB. 2006. Late Holocene sea-level changes and isostasy in western Denmark. Quaternary Research 66(2):288–302.

Gerlach MJ, Engelhart SE, Kemp AC, Moyer RP, Smoak JM, Bernhardt CE, Cahill N. 2017. Reconstructing common era relative sea-level change on the Gulf Coast of Florida. Marine Geology 390:254–269.

Haslett J, Parnell A. 2008. A simple monotone process with application to radiocarbon-dated depth chronologies. Journal of the Royal Statistical Society: Series C (Applied Statistics) 57(4):399–418.

Johnson BJ, Moore KA, Lehmann C, Bohlen C, Brown TA. 2007. Middle to late holocene fluctuations of $c_3$ and $c_4$ vegetation in a northern New England salt marsh, Sprague Marsh, Phippsburg Maine. Organic Geochemistry 38(3):394–403.

Kanawa T, Miyagi T, Fujimoto K, Kikuchi T. 1995. Late holocene sea-level changes and mangrove development in Kosrae Island, the Carolines, Micronesia. In: Kikuchi T, editor. Rapid sea level rise and mangrove habitat. Gifu, Japan: Institute for Basin Ecosystem Studies, Gifu University. p. 1–8.

Kemp AC, Bernhardt CE, Horton BP, Vane CH, Peltier WR, Hawkes AD, Donnelly JP, Parnell AC, Cahill N. 2014. Late Holocene sea- and land-level change on the U.S. Southeastern Atlantic Coast. Marine Geology 357:90–100.

Kemp AC, Hawkes AD, Donnelly JP, Vane CH, Horton BP, Hill TD, Anisfeld SC, Parnell AC, Cahill N. 2015. Relative sea-level change in

Connecticut (USA) during the last 2200 years. Earth and Planetary Science Letters 428: 217–229.
Kemp AC, Horton B, Donnelly JP, Mann ME, Vermeer M, Rahmstorf S. 2011. Climate related sea-level variations over the past two millennia. Proceedings of the National Academy of Sciences 108(27):11017–11022.
Kemp AC, Horton BP, Vane CH, Corbett DR, Bernhardt CE, Engelhart SE, Anisfeld SC, Parnell AC, Cahill N. 2013a. Sea-level change during the last 2500 years in new jersey, USA. Quaternary Science Reviews 81:90–104.
Kemp AC, Kegel JJ, Culver SJ, Barber DC, Mallinson DJ, Leorri E, Bernhardt CE, Cahill N, Riggs SR, Woodson AL et al. 2017. Extended Late Holocene relative sea-level histories for North Carolina, USA. Quaternary Science Reviews 160:13–30.
Kemp AC, Nelson AR, Horton BP. 2013b. Radiocarbon dating of plant macrofossils in tidal marsh sediment. In: Schroder J, editor. Treatise on geomorphology. San Diego, CA: Academic Press. p. 370–388.
Kemp AC, Vane CH, Horton BP, Culver SJ. 2010. Stable carbon isotopes as potential sea-level indicators in salt marshes, North Carolina, USA. The Holocene 20(4):623–636.
Kemp AC, Vane CH, Khan NS, Ellison JC, Engelhart SE, Horton BP, Nikitina D, Smith SR, Rodrigues LJ, Moyer RP. 2019. Testing the utility of geochemical proxies to reconstruct holocene coastal environments and relative sea level: a case study from Hungry Bay, Bermuda. Open Quaternary 5:1–17.
Kemp AC, Wright AJ, Edwards RJB, Brain M, Cahill N, Kopp RE, Horton BP, Charman DJ, Hawkes AD, Hill TD et al. 2018. Relative sea-level change in Newfoundland, Canada during the past ∼3000 years. Quaternary Science Reviews 201:89–110.
Kołaczek P, Gałka M, Lamentowicz M, Marcisz K, Kajukało-Drygalska K, Karpińska-Kołaczek M. 2019. Increased radiocarbon dating resolution of ombrotrophic peat profiles reveals periods of disturbance which were previously undetected. Quaternary Geochronology 52:21–28.
Kopp RE, Kemp AC, Bitterman K, Horton BP, Donnelly JP, Gehrels WR, Hay C, Mitrovica JX, Morrow E, Rahmstorf S. 2016. Temperature-driven global sea-level variability in the common era. Proceedings of the National Academy of Sciences 113(11):E1434–E1441.
Long AJ, Woodroffe SA, Milne GA, Bryant CL, Simpson MJR, Wake LM. 2012. Relative sea-level change in greenland during the last 700yrs and ice sheet response to the Little Ice Age. Earth and Planetary Science Letters 315–316:76–85.
Marshall W. 2015. Chronohorizons: Indirect and unique event dating methods for sea-level reconstructions. In: Shennan I, Long AJ, Horton BP, editors. Handbook of sea-level research. Wiley. p. 373–385.
Niering WA, Warren RS, Weymouth CG. 1977. Our dynamic tidal marshes: vegetation changes as revealed by peat analysis.
Parnell AC, Gehrels WR. 2015. Using chronological models in Late Holocene sea-level reconstructions from saltmarsh sediments. In: Shennan I, Long AJ, Horton BP, editors. Handbook of sea-level research. John Wiley & Sons. p. 500–513.
Parnell AC, Haslett J, Allen JRM, Buck CE, Huntley B. 2008. A flexible approach to assessing synchroneity of past events using bayesian reconstructions of sedimentation history. Quaternary Science Reviews 27(19-20): 1872–1885.
Peltier WR. 1996. Global sea level rise and glacial isostatic adjustment: an analysis of data from the east coast of North America. Geophysical Research Letters 23:GL00848.
Piecuch CG, Huybers P, Hay CC, Kemp AC, Little CM, Mitrovica JX, Ponte RM, Tingley MP. 2018. Origin of spatial variation in us east coast sea-level trends during 1900–2017. Nature 564(7736):400–404.
Redfield AC. 1972. Development of a New England salt marsh. Ecological Monographs 42(2): 201–237.
Reimer PJ, Austin WE, Bard E, Bayliss A, Blackwell PG, Ramsey CB, Butzin M, Cheng H, Edwards RL, Friedrich M. 2020. The Intcal20 Northern Hemisphere radiocarbon age calibration curve (0–55 cal kbp). Radiocarbon 62(4):725–757.
Roberts M, Elder K, Jenkins W, Gagnon A, Xu L, Hlavenka J, Longworth B. 2019. $^{14}$C blank corrections for 25–100 μg samples at the National Ocean Sciences AMS Laboratory. Radiocarbon 61(5):1403–1411.
Roberts ML, Burton JR, Elder KL, Longworth BE, McIntyre CP, von Reden KF, Han B, Rosenheim BE, Jenkins WJ, Galutschek E. 2010. A high-performance $^{14}$C accelerator mass spectrometry system. Radiocarbon 52(2): 228–235.
Scott DB, Williamson MA, Duffett TE. 1981. Marsh foraminifera of prince edward island: their recent distribution and application for former sea-level studies. Maritime Sediments and Atlantic Geology 17:98–129.
Sefton J, Woodroffe S, Ascough P. 2021. Radiocarbon dating of mangrove sediments. In: Sidik F, Friess DA, editors. Dynamic sedimentary environments of mangrove coasts. Elsevier. p. 199–215.
Stuiver M, Polach HA. 1977. Reporting of $^{14}$C data. Radiocarbon 19(3):355–363.
Swindles GT, Blundell A, Roe HM, Hall VA. 2010. A 4500-year proxy climate record from peatlands in the north of ireland: The identification of widespread summer 'drought

phases'? Quaternary Science Reviews 29(13): 1577–1589.
van de Plassche O, van der Borg K, de Jong AFM. 1998. Sea level-climate correlation during the past 1400 yr. Geology 26(4):319–322.
Vogel JS, Southon JR, Nelson DE. 1987. Catalyst and binder effects in the use of filamentous graphite for ams. Nuclear Instruments and Methods in Physics Research Section B: Beam Interactions with Materials and Atoms 29(1):50–56.
Walker JS, Kopp RE, Shaw TA, Cahill N, Khan NS, Barber DC, Ashe EL, Brain MJ, Clear JL, Corbett DR et al. 2021. Common era sea-level budgets along the U.S. Atlantic coast. Nature Communications 12(1):1841.
Wang X-C, Chen R, Berry A. 2003. Sources and preservation of organic matter in plum island salt marsh sediments (MA, USA): long-chain n-alkanes and stable carbon isotope compositions. Estuarine, Coastal and Shelf Science 58(4): 917–928.
Woodroffe SA, Long AJ, Milne GA, Bryant CL, Thomas AL. 2015a. New constraints on Late Holocene eustatic sea-level changes from Mahé, Seychelles. Quaternary Science Reviews 115:1–16.
Woodroffe SA, Long AJ, Punwong P, Selby K, Bryant CL, Marchant R. 2015b. Radiocarbon dating of mangrove sediments to constrain Holocene relative sea-level change on zanzibar in the southwest indian ocean. The Holocene 25(5):820–831.
Wright AJ, Edwards RJ, van de Plassche O, Blaauw M, Parnell AC, van der Borg K, de Jong AF, Roe HM, Selby K, Black S. 2017. Reconstructing the accumulation history of a saltmarsh sediment core: Which age-depth model is best? Quaternary Geochronology 39:35–67.